

A Stable Graphite Negative Electrode for the Lithium-Sulfur Battery

Fabian Jeschull, Daniel Brandell, Kristina Edström, Matthew J. Lacey

*Department of Chemistry - Ångström Laboratory, Uppsala University, Box 538,
Lägerhyddsvägen 1, 75121 Uppsala, Sweden*

Supporting Information

Experimental details

Materials

Porous polyethylene (Solupor, Lydall Performance Materials) separators were dried overnight at 80° C under vacuum. Lithium nitrate (Aldrich) and lithium bis-trifluoromethanesulfoimide (LiTFSI, Novolite) were dried at 120 °C overnight. 1,2-dimethoxyethane (DME, Novolyte) and 1,3-dioxolane (DOL, anhydrous, Aldrich) were used as received and mixed in a ratio of 1:1 by volume.

Poly(vinylene difluoride-hexafluoropropylene) (PVdF-HFP, Kynar FLEX 2801, Arkema) was dissolved beforehand in N-methylpyrrolidone (NMP, Aldrich) to yield a 5 wt.% solution. A 35 wt.% solution of poly(acrylic acid) (PAA, $M_w = 450,000$, Aldrich, 35 wt.% aqueous solution) was deprotonated with a 4 M aqueous NaOH (Aldrich) solution to give a 15 wt.% PAA-Na binder solution. Carboxymethyl cellulose sodium salt (CMC-Na, degree of substitution: 0.79) was kindly provided by Dow Chemicals and used as received.

Electrode and electrolyte preparation

The graphite electrode slurries comprised 85 wt.% coarse graphite powder (Leclanché, average particle size > 10 μm), 3 wt.% fine graphite powder (KS6, Imerys, particle size <7 μm), 2 wt.% conductive additive (Super C65, Imerys) and 10 wt.% binder. The powders were dispersed in either NMP (PVdF-HFP) or H₂O (CMC-Na, PAA-Na), respectively. The viscosity of the slurry was adjusted with addition of a corresponding amount of solvent. The slurry was mixed by planetary ball milling for 2h and then bar casted on copper foil (Goodfellow, 22 μm thick). After drying at 60 °C (NMP) or ambient conditions (H₂O) the electrodes were punched into 13 mm and 20 mm discs, respectively, transferred to an Ar-

filled glovebox and dried under vacuum at 80 °C for 12 h. Graphite loadings varied between 4.1 – 4.8 mg graphite per cm².

A sulfur-KB composite (w/w = 58:28) was prepared by melt infiltration prior to slurry preparation. The two powders were blended in a mortar and then heated in a Buchi furnace to 155 °C for 20 min. The sulfur composite electrodes consisted of 58 wt.% sulfur (Aldrich), 28 wt.% Ketjen Black EC-600JD (KB, Akzo Nobel), 7 wt.% Super C65, 5 wt.% styrene-butadiene rubber (SBR) and 2 wt.% CMC-Na. The slurry was ball-milled for 2h in a planetary ball mill and then bar casted on aluminum foil (Goodfellow, 19 μm thick). The coated electrode was dried under ambient conditions, punched into 13 mm discs and subjected to further drying under vacuum in an Ar-filled glovebox for 12 h at 60° C. Sulfur loadings varied between 0.6 and 0.75 mg sulfur per cm².

Two electrolyte formulations were applied in this study: 1 M LiTFSI and 0.25 M LiNO₃ were dissolved in a mixture of DME:DOL (v/v = 1:1) (referred to as standard electrolyte). The second formulation contained 1 M LiTFSI electrolyte salt only.

Cell assembly

Graphite electrodes (20 mm discs) were first tested in half cells against lithium metal in a pouch cell format with copper current collectors. A circular Celgard separator (diameter 25 mm) was wetted with 75 μL of either the standard electrolyte or an electrolyte solution without LiNO₃. A piece of lithium foil (125 μm thick, Cyprus Foote Mineral) of about the size of the separator was used as counter electrode.

Lithium-sulfur and lithiated graphite-sulfur batteries were examined in 2520 coin cells. Lithium-sulfur batteries were assembled in dry state with a circular Celgard separator (diameter 17 mm) and lithium foil (diameter 15 mm). The thickness of the lithium foil was 30 μm (“thin lithium foil”, Rockwood Lithium) or 125 μm (“thick lithium foil”), respectively.

Because of the high vapor pressure of the electrolyte solvents, the standard electrolyte (7 μL/mg sulfur) was added as the last component before the coin cell was sealed.

Lithiation of graphite electrodes (13 mm discs) was carried out in a pouch cell against lithium foil (125 μm) with copper current collectors. A circular Celgard separator (20 mm) was wetted with 75 μL standard electrolyte. The lithium foil was cut in squared shape of about the same size as the separator. After lithiation (see protocol below) the pouch cell was opened in the glovebox and used as counter electrode against a sulfur positive electrode (coin cell format). Electrolyte volumes and separator size were similar to the lithium-sulfur coin cell assembly described above. Two experiments were carried out with thick lithium foil in

circular shape (diameter 15 mm). After the charging procedure, the cycled foil was used as counter electrode in a conventional lithium-sulfur cell (coin cell format, as described above).

Electrochemical measurements

Galvanostatic cycling and self-discharge experiments were performed on an Arbin BT-2043 battery cycler. Graphite half cells were cycled at a rate of $C/10$ ($C = 372 \text{ mAh g}^{-1}$) within the voltage limits of 5 mV and 1.5 V. For the galvanostatic cycling of lithium/graphite half-cells the capacity was limited to a maximum of 350 mAh g^{-1} . Graphite electrodes for use in graphite-sulfur cells were cycled for 6 or 9 cycles without capacity limitation. Pouch cells were clamped between two plates to maintain a constant stack pressure during the measurements.

For the following cycling procedures, the cycling rate was referred to the capacity of the sulfur electrode ($1 C = 1672 \text{ mAh g}^{-1}$). Lithium-sulfur cells were cycled in the voltage range of 1.8 – 2.6 V at a rate of $C/10$. For graphite-sulfur cells, the lower cut-off limit was 100 mV lower in order to account for the higher redox potential of graphite vs. lithium. Graphite-sulfur cells were also cycled at $C/20$ for the first cycle only as this was found to ensure repeatable behaviour on continued cycling.

To measure self-discharge, cells were cycled at a constant rate of $C/10$ and stopped in the charged state every three cycles. The cell was allowed to rest at OCV for time periods of 12, 24, 72, 168 and 336 hours. Following the resting period cycling was re-commenced. The difference in the discharge capacity following the long OCV period allows for evaluation of the rate of self-discharge.

Supplementary data

Stability test of various graphite-lithium half-cells

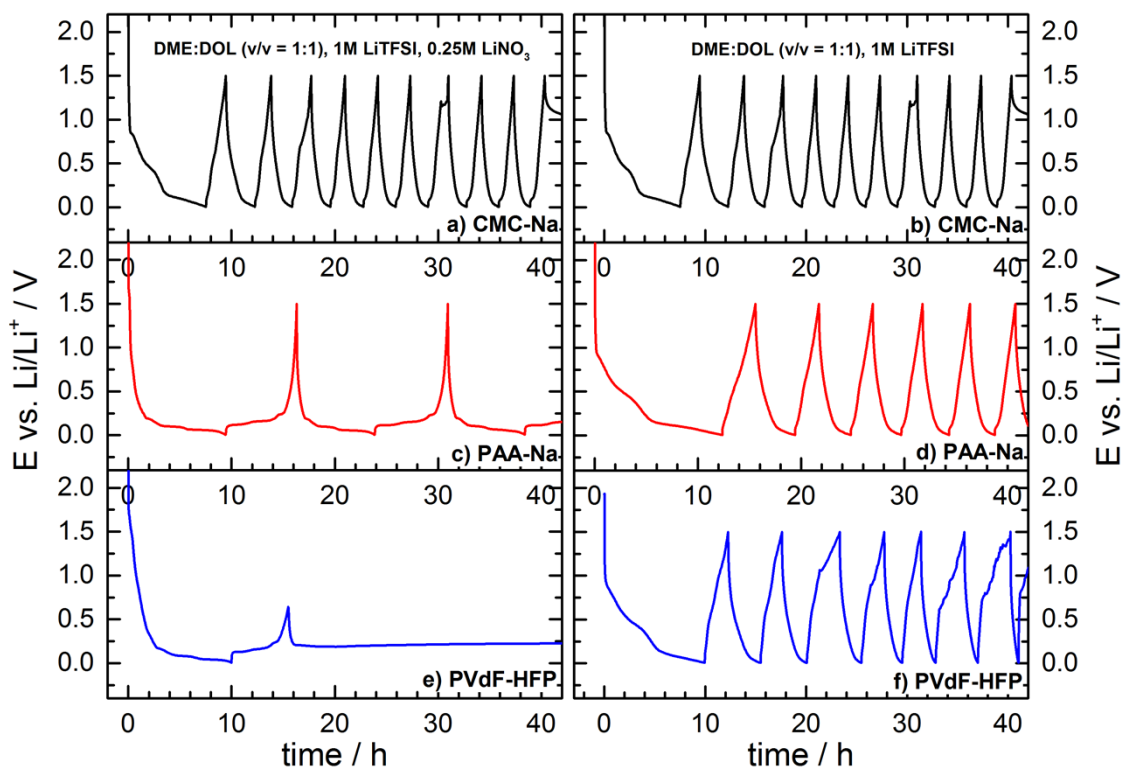


Fig. S1: Voltage profiles of graphite-lithium half-cells containing CMC-Na (top row, a) & b)), PAA-Na (middle row, c) & d)) and PVdF-HFP (bottom row, e) & f)) as electrode binder, respectively. The left column shows cells cycled in a standard electrolyte formulation comprising DME:DOL (v/v = 1:1), 1M LiTFSI and 0.25M of the electrolyte additive LiNO₃. In the right column the cells were cycled without the electrolyte additive under similar conditions.

Voltage profiles for lithium-sulfur and graphite-sulfur cells

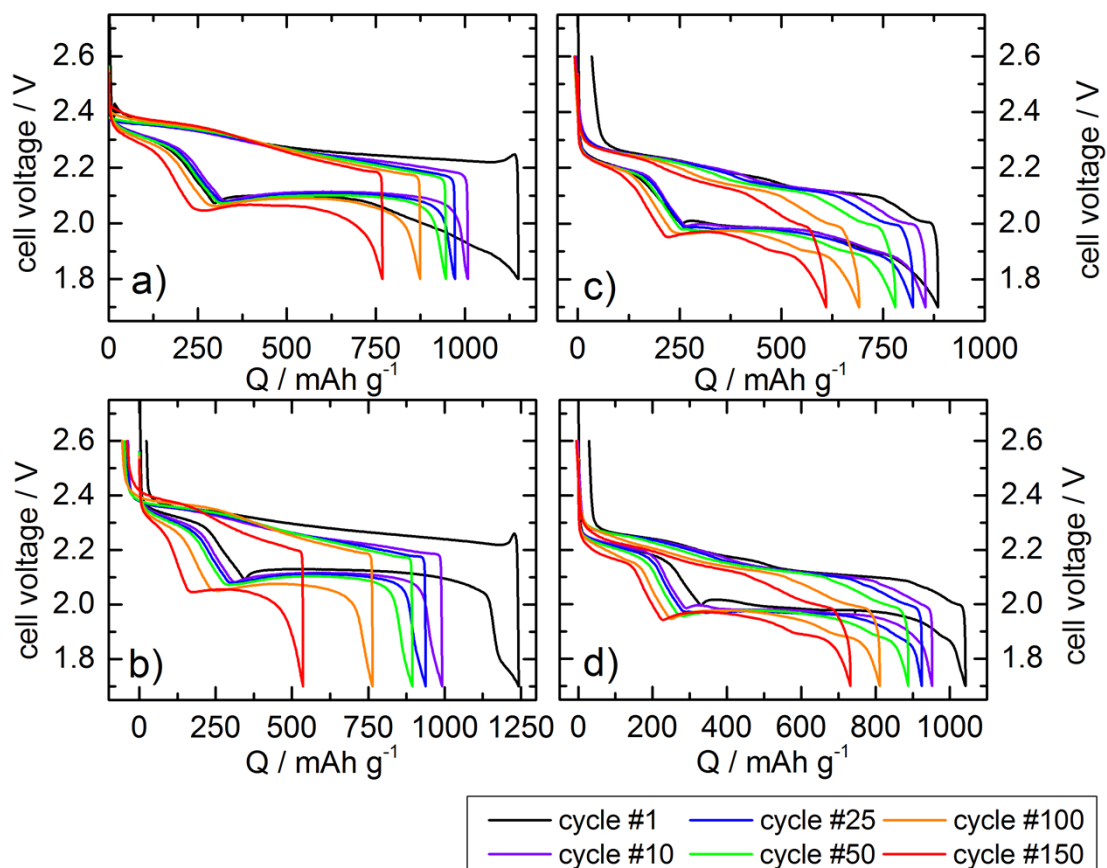


Figure S2: Voltage profiles for cells described in the manuscript on selected cycles. a) Lithium-sulfur cell with a thick Li anode, b) lithium-sulfur cell with a thin Li anode, c) graphite-sulfur cell with a graphite anode pre-cycled for 6 cycles, d) graphite-sulfur cell with a graphite anode pre-cycled for 9 cycles.

Changes in cell resistance

In the cycling program used in this work, cells are switched to OCV for 10 seconds between charge and discharge steps. At each charge and discharge limit, cell resistance can be estimated as $R = dE/dI$ from the voltage drop when the current is switched off (the time difference between the first data point of the OCV period and the last data point of the current step from which the voltage drop is calculated is 1 second). This allows for a rough estimate of the change in cell resistance over the duration of the experiment.

The results of this analysis are presented in Figure S3. Both graphite cells show relatively stable resistances over the duration of the experiment, with a slightly higher average resistance for the cell where the anode was pre-cycled for 9 cycles instead of 6. Both cells with Li metal anodes show a continuous increase in the resistance, with the rate of increase more severe for the cell with a thin Li metal anode.

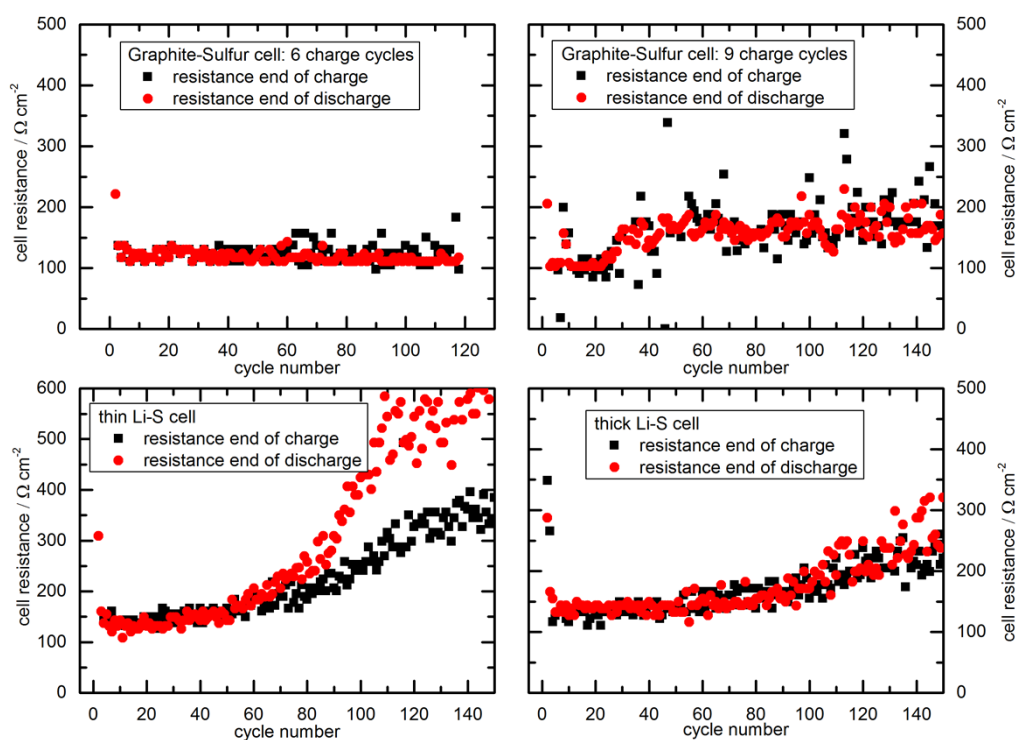


Fig. S3: Cell resistances for two graphite-sulfur cells and two Li-S cells comprising thin and thick lithium foil respectively. Cell resistances were measured at the end of every charge and discharge sequence.